



# Double Yielding in Deformation of Semicrystalline Polymers

Masoud Razavi\* and Shi-Qing Wang

Different semicrystalline polymers including poly(L-lactic acid), poly(ethylene terephthalate), syndiotactic polystyrene, and polyamide 12 are studied in terms of their mechanical response to uniaxial compression deformation. Apparent decoupling of yielding of amorphous and crystalline phases is identified as separate peaks in the stress–strain curve in the vicinity of the glass transition temperature. The same feature is also observed for the uniaxial extension of predrawn semicrystalline poly(ethylene terephthalate). It is indicated that in absence of a strong amorphous phase a semicrystalline polymer is unable to yield and undergo plastic deformation and it fails in a brittle manner in the uniaxial compression. Treating a semicrystalline polymer as a composite of amorphous and crystalline phases, putting emphasis on the crucial role of amorphous phase in acting as connectors between crystalline domains and indicating that the yielding of amorphous phase is a prerequisite for yielding of crystalline phase, work toward a better understanding of the mechanical properties of semicrystalline polymers at the molecular level is done.

## 1. Introduction

A semicrystalline polymer, at a specific temperature, depending on the positive or negative distance from glass transition temperature ( $T_g$ ) of amorphous phase, can be treated as a composite of glassy and crystalline phases (at  $T < T_g$ ) or melt and crystalline phases (at  $T > T_g$ ). Because of structural complexity of semicrystalline polymers, and incomplete understanding of preceding studies about the molecular mechanics of glassy polymers and nonlinear rheology, study of mechanics of these class of polymers at the “molecular level” remains as one of the most challenging areas in polymer physics. Meanwhile, due to the practical importance of semicrystalline polymers especially polyolefins such as polyethylene and polypropylene, at the “continuum level” tremendous efforts have been paid to model the stress–strain behavior of those polymers.<sup>[1–7]</sup> These

studies ignored the crucial role of the amorphous phase in delivering required force and chain tension into the crystalline phase in order to disintegrate it, and mainly focused on modeling the stress–strain curves or characterize the changes in crystalline structure.<sup>[8–13]</sup> However, the right strategy to tackle this elusive problem, i.e., molecular mechanics of semicrystalline polymers, should be a bottom up approach that first understands melt rheology and molecular mechanics of pure glassy phase and in the next stage by incorporating crystalline phase into the disordered phase tries to perceive the effects of crystalline phase on the mechanical performance of the resultant composite system. In this regard, study of semicrystalline polymers with higher  $T_g$  than room temperature such as polyesters; e.g., poly(L-lactic acid) (PLLA) and poly(ethylene terephthalate) (PET), could be more useful in providing

suitable model polymers that are able to be quenched below  $T_g$  and produce amorphous counterparts as control samples. Another benefit with these polymers is that we are able to easily study the mechanical behavior both below and above  $T_g$ . Previous studies by Flory<sup>[14]</sup> and Peterlin<sup>[15,16]</sup> tried to understand the yielding of semicrystalline polymers by characterizing the changes of crystalline phase in presence of stress. More recent studies by Strobl<sup>[17,18]</sup> on semicrystalline polymers with high  $T_g$  treated the crystalline phase as a force-transmitting skeleton. Unlike preceding studies, the objective of this paper is to understand the semicrystalline state as a composite structure of amorphous and crystalline phases by focusing on the imperative role of amorphous phase in connecting crystalline regions to one another and providing local stress exerted on crystalline regions to cause yielding to occur in the crystalline phase. The importance of chain networking in amorphous phase, and interaction of amorphous phase with crystalline phase in delivering mechanical input into crystalline regions are highlighted in our study. Based on the new framework, for the first time, to the best of authors’ knowledge, the brittle response of a semicrystalline polymer under compression deformation is predicted and experimentally demonstrated in this study. We demonstrate that the effective deformation of crystalline phase is impossible in absence of a robust amorphous phase. In other words, based on our results that is the amorphous phase, which its deformation generates

Dr. M. Razavi, Prof. S.-Q. Wang  
Department of Polymer Science  
University of Akron  
Akron, OH 44325, USA  
E-mail: mr161@zips.uakron.edu

The ORCID identification number(s) for the author(s) of this article can be found under <https://doi.org/10.1002/macp.202000151>.

DOI: 10.1002/macp.202000151

**Table 1.** Molecular characteristics of various semicrystalline samples.

Polymer	$M_w$ [kg mol <sup>-1</sup> ]	$M_e$ [kg mol <sup>-1</sup> ]	$T_g$ [°C]	Source
PLLA	115	3.24	60	Nature Works (Ingeo 3100HP)
PET	–	1.45	80 (77)	Eastman (7352 PET)
sPS	175	2.44	100 (93)	Idemitsu Kosan (130ZC)
PA 12	–	1.6–2.6	36	RTP Company (RTP 200F)

local stress to make yielding of crystalline phase possible and the crystalline phase cannot yield independently.

## 2. Experimental Section

### 2.1. Materials

Four commercial semicrystalline polymers including PLLA, PET, syndiotactic polystyrene (sPS), and polyamide 12 (PA 12) are used in this study. The weight average molecular weight  $M_w$ , entanglement molecular weight  $M_e$ , and glass transition temperature  $T_g$  of these polymers are listed in **Table 1**. The  $T_g$  values of these polymers were obtained using Discovery DSC 2500 (TA instruments) from heating cycle when the samples were heated with the rate of 5 °C min<sup>-1</sup>. For each sample  $T_g$  was measured two times; when the sample is heated up from fully amorphous state and also in the second heating cycle when the sample had been partially crystallized in the first cooling. In the case of PLLA and PA 12 the two values are equal; however, for PET and sPS the  $T_g$  of partially crystallized sample is slightly higher than  $T_g$  of fully amorphous counterpart. For these polymers, i.e., PET and sPS, the  $T_g$  of fully amorphous sample is presented in parentheses in Table 1.

Gel permeation chromatography (GPC) measurements of crystalline PLLA, PLLAc, and thermally treated PLLAc, tPLLA—more details about this sample are provided in the discussion section—were carried out using THF-based GPC equipped with Wyatt Dawn Eos multiangle laser light (MALLS) detector and Waters Model 2414 differential refractometer concentration detector. The weight average molecular weights of PLLAc and tPLLA were obtained to be equal to 108 and 47 kg mol<sup>-1</sup>, respectively.

### 2.2. Sample Preparation

In order to remove moisture from polymer pellets they were initially dried in temperature-controlled chamber (Thelco GCA Precision model 18) for few hours. For the uniaxial compression tests, cylindrical samples with the diameter and height of 5 mm were made from compression molding of resin pellets using a Carver Lab Press. The applied load during molding was equal to 9000 kg. In the case of PLLA and PET polymer resins were melted above their melting point of 190 and 290 °C respectively and then after waiting for few minutes they were quickly quenched into a icy water to generate amorphous PLLA and PET. In the next stage the amorphous PLLA and PET

cylinders were annealed in the temperature-controlled chamber respectively at 90–100 and 150–160 °C for 4 h to prepare semicrystalline samples of PLLA and PET. Semicrystalline sPS and PA 12 samples were prepared by slow cooling from melt state toward room temperature during which melt crystallization took place. Dog-bone samples of semicrystalline PLLA and PET with dimensions of length by width by thickness respectively equal to 10 × 2.9 × 1.35 mm<sup>3</sup> were prepared using dog-bone shape mold and similar molding and annealing conditions to those of corresponding compression pieces.

### 2.3. Mechanical Measurements

Uniaxial compression tests of cylindrical samples were carried out using Instron 5969, equipped with an environmental chamber. The temperature controller for Instron has an accuracy of ±1 °C. The tests were conducted over a range of temperatures covering  $T_g$ . Bluehill Software interfaced with Instron allows to perform compression tests with various constant crosshead speeds  $V$  in the unit of mm min<sup>-1</sup>, which were then normalized by initial height  $H_0$  to indicate the compression rate  $r = V/H_0$  (min<sup>-1</sup>). Compression rate for all the measurements was set equal to 0.33 min<sup>-1</sup> in order to prevent heat generation in sample and retain isothermal condition. All cylinder-shaped specimens were well lubricated on top and bottom surface with silicone oil. Uniaxial extension of semicrystalline PET at 20 and 100 °C, and semicrystalline PLLA at  $T = 20$  °C were performed using the same Instron. Drawing rate  $V/L_0$  where the  $V$  is the crosshead separation speed and  $L_0$  is initial length of sample was set to be 0.5 min<sup>-1</sup>. **Figure 1** indicates that semicrystalline PLLA and PET are brittle when they are extended below  $T_g$ ; however, same PET when it is drawn at  $T = 100$  °C shows a ductile behavior. After extension of the semicrystalline PET above  $T_g$ , the necked part of sample was further stretched at room temperature and the stress versus strain curve was represented in **Figure 6**.

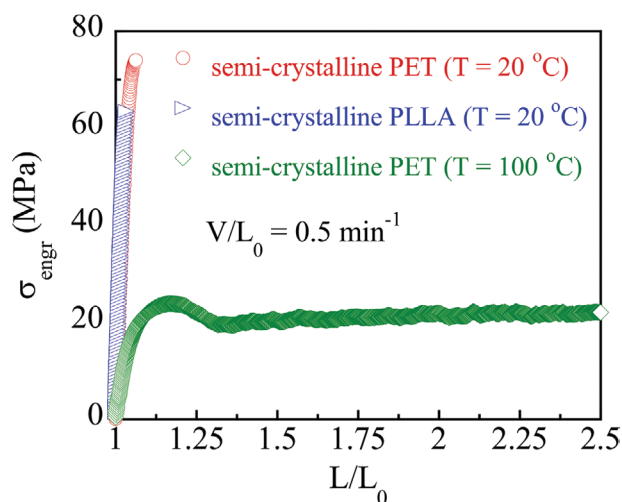


**Figure 1.** Engineering stress  $\sigma_{\text{engr}}$  versus draw ratio  $L/L_0$  for the uniaxial tensile deformation of semicrystalline PET at two temperatures of 20 ° and 100 °C, and semicrystalline PLLA at 20 °C.

#### 2.4. Wide-Angle X-Ray Scattering (WAXS) Measurements

2D WAXS patterns were obtained using a rotating anode X-ray generator (RU 300, 12 kW, Rigaku, Woodlands, TX), which produced a beam of monochromatic Cu  $K\alpha$  radiation ( $\lambda = 1.54 \text{ \AA}$ ). The X-ray generator operates at 40 kV and 30 mA.

### 3. Results and Discussion

Crystalline PLLA and PET are brittle when they are extended below  $T_g$  (Experimental section, Figure 1). Therefore, initially we start our discussion with the uniaxial compression of these polymers when they show a ductile behavior. The explanation of why semicrystalline PLLA is brittle below  $T_g$  in extension, was presented in detail in our previous publication.<sup>[19]</sup> Also the reason behind why the same semicrystalline polymer which is brittle in extension could turn ductile in compression is the subject of our future study.<sup>[20]</sup> Here we only focus on importance of understanding semicrystalline state as a composite structure and the crucial role of amorphous phase in exerting deformation on crystalline phase. **Figure 2** compares the stress  $\sigma$  versus compression ratio  $H_0/H$  of cold crystallized PLLA, PLLAc, and its counterpart amorphous sample PLLAa which was produced by fast quenching of PLLA melt below  $T_g$  (60 °C), at room temperature.

Evidently, it is seen that incorporation of crystalline phase into the amorphous one results in increase of yield stress which could be due to the rigid nature of crystalline phase. However, it is a valid question to ask that what does happen

at yield point in each case (PLLAa and PLLAc)? What is/are the difference(s) in yielding of amorphous and semicrystalline polymers? According to our recent molecular model,<sup>[21]</sup> yielding of a glassy polymer (polymer glass) is defined as activation of chain network associated with increase in the segmental mobility and it turns out that the condition for activation of chain network is more readily provided in compression deformation compared to tensile deformation.<sup>[22,23]</sup> Considering a semicrystalline polymer as a composite structure of glassy and crystalline phases below  $T_g$ , we predict that the yielding of a semicrystalline polymer should involve two yielding, yielding of glassy phase followed by yielding of crystalline phase. Yielding of glassy phase should not be different than that of a pure glassy polymer, on the other hand yielding of crystalline phase is due to destruction of crystalline structure which itself can be combination of “fragmentation” and “force-induced melting”. Both mechanisms result in reduction of crystallinity which in the recent example it is evidenced using the 2D WAXS images. Fragmentation is the mechanism of destruction of crystals which presumably does not require strong chain networking in amorphous phase, while force-induced melting of crystals is a mechanism wherein the nominal deformation initially translates to the amplified chain tension in the amorphous phase, and subsequently through bridging and tie chains is exerted onto the crystalline lamellae, and pulls the whole or portion of the chains out of the crystalline lamellae, and in absence of recrystallization at  $T < T_g$  results in reduction of overall crystallinity. Yielding of crystalline phase is evidenced by the 2D images from WAXS; however, there is no direct or indirect evidence that can unveil the yielding of glassy phase in Figure 2. Higher mobility and relative motion of segments are achieved in an amorphous glassy polymer by approaching yield point,<sup>[24,25]</sup> therefore for a glassy amorphous polymer yield stress can be an indicator of the strength of intersegmental interactions. On the other hand, in an analogy with the molecular crystals,<sup>[26]</sup> the strength of crystalline phase of a polymeric material can be evaluated by the amount of cohesive energy (binding energy) which is indication of the strength of intermolecular interactions in the crystalline phase. Overcoming this intermolecular interaction and increasing the potential energy of crystalline phase above its equilibrium energy state, i.e., cohesive energy, provides the conditions to destruct the crystalline structure, i.e., yielding of crystalline phase. The yield stress of glassy polymer  $\sigma_{yg}$  and cohesive energy density  $CED_c$  of crystalline phase (note the same dimensionality of  $[M T^{-2} L^{-1}]$  for these parameters), both are decreasing functions regarding temperature (**Figure 3**). Passing  $T_g$ ,  $\sigma_{yg}$  sharply drops to the order of plateau modulus of melt  $G_0$ , while in principle  $CED_c$  is insensitive to  $T_g$  and gradually decays and reaches its value for the melt by going beyond melting temperature  $T_m$ . Therefore, we predict that near  $T_g$  is the temperature range where the contrast between strength of these two phases is large and that could result in apparent decoupling of yielding of glassy and crystalline phases. To validate this prediction, compression of PLLAc was done in four different temperatures and curves of  $\sigma$  versus  $H_0/H$  were examined in a higher magnification around the stress maximum in **Figure 4**.

Interestingly as predicted, near  $T_g$  the two yielding appear as two individual peaks in the stress versus strain curves. Because

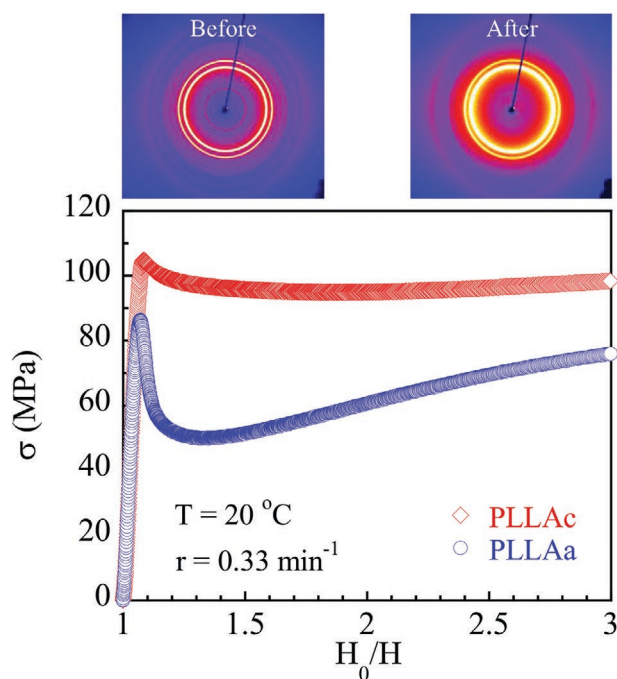


**Figure 2.** Stress  $\sigma$  versus compression ratio  $H_0/H$  curves for the uniaxial compression of semicrystalline PLLA (PLLAc) and its amorphous counterpart PLLAa at  $T = 20 \text{ }^\circ\text{C}$ . 2D-WAXS images at left (before deformation) and right (after deformation) indicate the reduction in crystallinity at postyield for PLLAc.

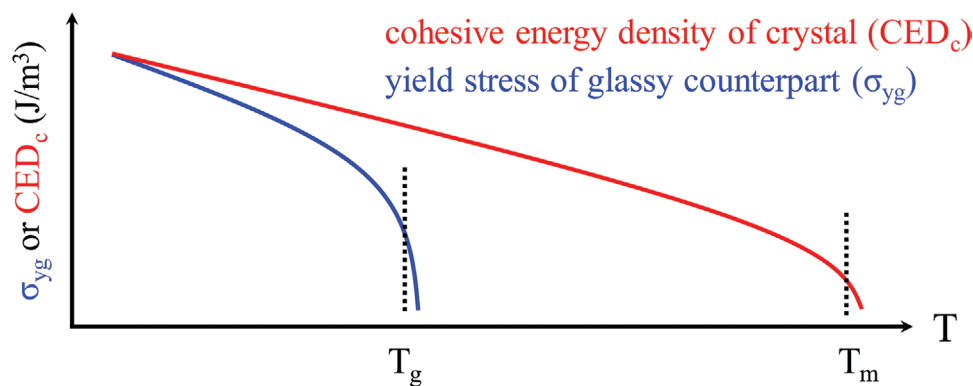


**Figure 3.** Diagram showing changes in the strength of pure glassy and pure crystalline phases in terms of yield stress ( $\sigma_{yg}$ ) and cohesive energy density ( $CED_c$ ), respectively.

of higher segmental mobility of amorphous phase and amplification effect in deformation of this phase,<sup>[19]</sup> the earlier peak has to associate with the yielding of amorphous phase and the second one should be related to the yielding of crystalline phase. In other words, in order to crystalline phase to be able to yield it requires that initially the amorphous phase to yield and develop enough chain tension, so the developed high chain tension can act on the crystalline regions and result in yielding of crystalline phase. At the higher temperatures (Figure 4d), amorphous phase is in the melt state and does not show mechanical

resistance against deformation. Therefore, sample is compressed until the point where chain tension is high enough to start to pullout the chains from crystal registrars. On the other hand, far below  $T_g$ , since the glassy modulus is temperature-independent and yield stress increases by decreasing temperature; therefore, the strain to yield of glassy phase increases by lowering temperature. Meanwhile, it is seen that the position of the second yield in Figure 4b,c is independent of temperature. Accordingly, at the lower temperatures (Figure 4a) the first yield from glassy phase which occurs at higher compression

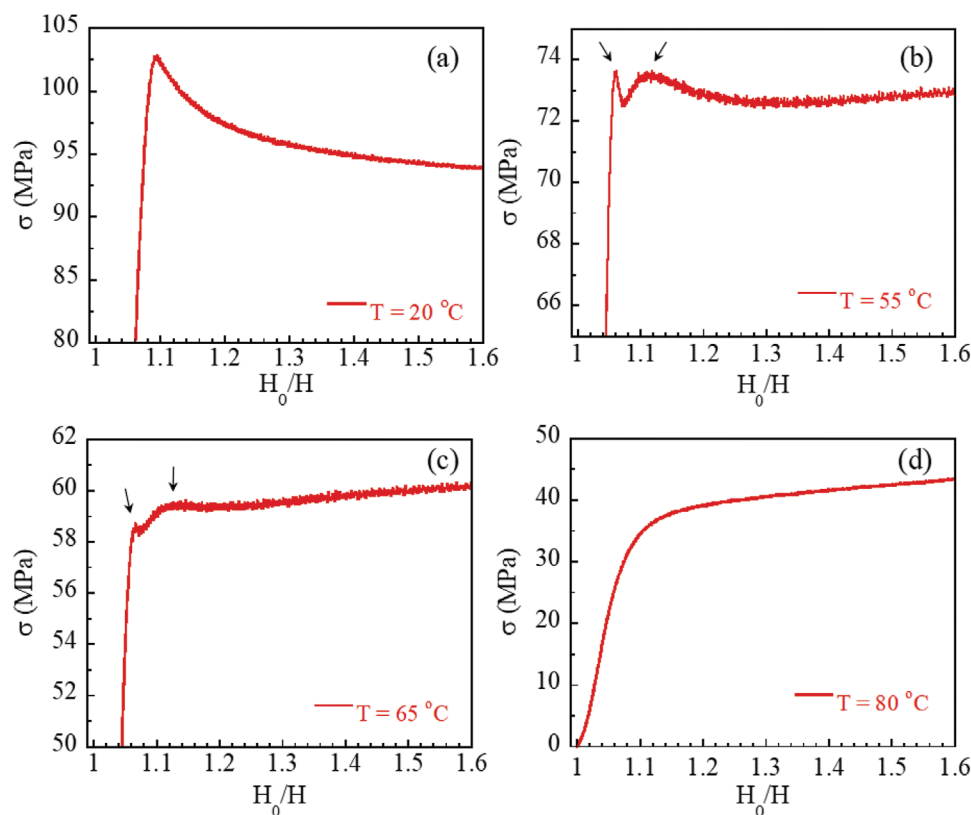


**Figure 4.** Stress  $\sigma$  versus compression ratio  $H_0/H$  curves for the uniaxial compression of PLLAc in the vicinity of stress maximum at a)  $T = 20\text{ }^\circ\text{C}$ , b)  $T = 55\text{ }^\circ\text{C}$  ( $T_g - 5$ ), c)  $T = 65\text{ }^\circ\text{C}$  ( $T_g + 5$ ), and d)  $T = 80\text{ }^\circ\text{C}$ . For all the measurements compression rate was  $0.33\text{ min}^{-1}$ . Apparent decoupling of glassy and crystalline yields appears near  $T_g$  (indicated by arrows), while such effect is absent far above and far below  $T_g$ .



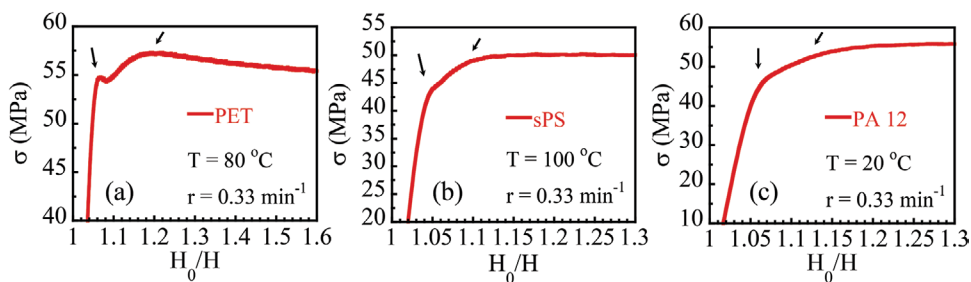


**Figure 5.** Stress  $\sigma$  versus compression ratio  $H_0/H$  curves for the uniaxial compression of semicrystalline a) PET ( $T_g = 80\text{ }^\circ\text{C}$ ), b) sPS ( $T_g = 100\text{ }^\circ\text{C}$ ), and c) PA 12 ( $T_g = 36\text{ }^\circ\text{C}$ ) in the vicinity of yield points indicating double yield, i.e., apparent decoupling of glassy and crystalline yields (indicated by arrows).

ratios, merges out with the peak associated with the yield of crystalline phase and apparently, we only observe one unified but wide peak having minor strain softening. To have an easier comparison among the compression behavior of PLLAc in different temperatures, the Figure 4a–d are plotted in a same scale in Figure S1 in the Supporting Information.

To determine whether these observations are universal, we carried out uniaxial compression of PET, sPS and PA 12 at different temperatures. Similarly, in all the cases, away from  $T_g$  an apparent yield point with a single peak is observed while close to  $T_g$  splitting of the yield points takes place. **Figure 5a–c** represents the curves of near- $T_g$  effect for these three semicrystalline polymers.

In passing we are interested to show the presence of double yielding in the tensile deformation of semicrystalline polymers below  $T_g$ . It turns out that predrawing of a semicrystalline polymer above  $T_g$  makes it ductile when it is further drawn below  $T_g$ .<sup>[27]</sup> **Figure 6** represents the engineering stress  $\sigma_{\text{engr}}$  versus draw ratio  $L/L_0$  during tensile deformation of predrawn semicrystalline PET at  $T = 20\text{ }^\circ\text{C}$  when it is deforming parallel to the stretching direction. As it is seen predrawn semicrystalline PET shows two yield points (indicated by arrows). The preceding discussions indicated the universality of double-yielding phenomenon for various modes of deformation, i.e., compression and extension, and different types of semicrystalline polymers, i.e., PLLA, PET, sPS and PA 12.

In the next stage in order to reiterate the important role of tie chains and chain networking in amorphous phase, in affording the required force to yield the crystalline phase we design following experiment. Amorphous portions of the chains were selectively degraded by maintaining a semicrystalline compression piece of PLLAc at high temperature  $\approx 140\text{--}150\text{ }^\circ\text{C}$  for 100 h. Molecular weight  $M_w$  measurements based on gel permeation chromatography GPC indicated that after this treatment the overall molecular weight changes from 108 to 47  $\text{kg mol}^{-1}$ . The molecular weight  $M_w$  after degradation (47  $\text{kg mol}^{-1}$ ) is still far above entanglement molecular weight  $M_e$  of 3.24  $\text{kg mol}^{-1}$ ,<sup>[19]</sup> however, the response of semicrystalline polymer to the uniaxial compression changed from ductile to a brittle one (**Figure 7**) upon this thermal treatment. This indicates that degradation mostly took place in the amorphous phase of the semicrystalline sample. Thermal treatment results in degradation in amorphous phase and that phase no longer is able to yield and deliver the force to the crystalline phase. Because of the noneffective chain networking in the amorphous phase,

high chain tension cannot establish and survive for a long time, so chain pull out in amorphous phase takes place before that phase has the chance to exert the required force on the crystalline phase and result in yielding of that phase and this is why the WAXS images of treated semicrystalline PLLA, tPLLAc before and after compression remains unchanged. Moreover, a new amorphous cylindrical specimen for compression experiment was prepared by melting and fast quenching of the thermally treated semicrystalline tPLLAc piece, and labeled as reprocessed amorphous PLLA, rpPLLAA. Conceivably, rpPLLAA shows a ductile behavior under uniaxial compression test. These set of experiments indicated that during treatment process we were able to selectively degrade the tie and bridging chains in the amorphous regions, so the chain networking in the amorphous phase is no longer effective enough to result in yielding of glassy phase and generate high chain tension and subsequently drives the crystalline phase to undergo yielding, meanwhile the overall molecular weight is high enough that rpPLLAA prepared by remelting of treated sample, still remains ductile. It is necessary to point out that like below  $T_g$ , above  $T_g$ , those should be the highly strained amorphous chains that input the force on the crystalline regions to derive them toward yielding though force-induced melting.

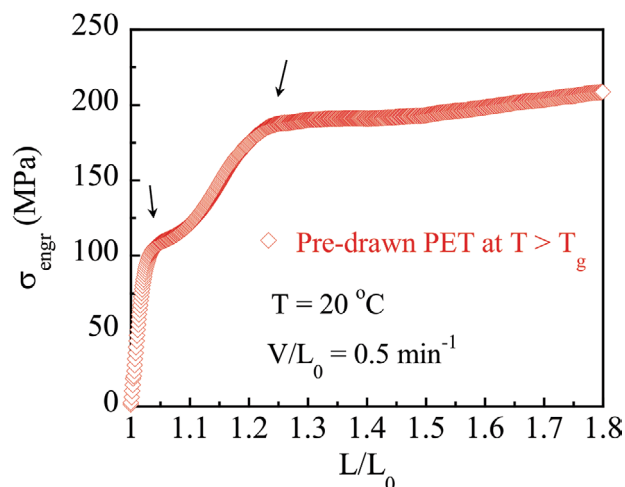


**Figure 6.** Engineering stress  $\sigma_{\text{engr}}$  versus draw ratio  $L/L_0$  during the tensile deformation of predrawn crystalline PET, at  $T = 20\text{ }^\circ\text{C}$  when it is deforming parallel to the stretching direction. Arrows indicate presence of two yield points. Predrawing of crystalline PET was performed at  $100\text{ }^\circ\text{C}$ .

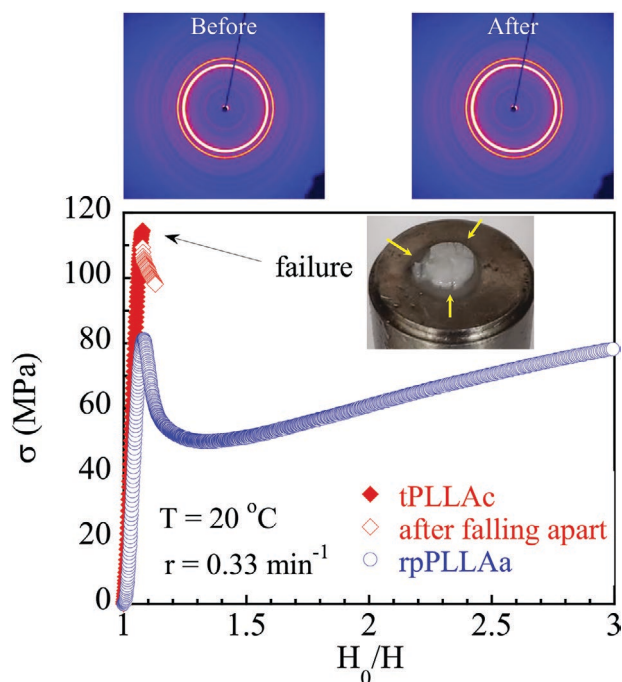


**Figure 7.** Stress  $\sigma$  versus compression ratio  $H_0/H$  curves for the uniaxial compression of thermally treated crystalline PLLA, tPLLAc, and its counterpart amorphous sample after melting and fast quenching of tPLLAc to room temperature, labeled as reprocessed amorphous PLLA, rpPLLAc. Inset image shows the brittle behavior of tPLLAc. No change in 2D-WAXS image of tPLLAc after compression indicates that the crystalline phase is unable to yield independently in absence of an effective robust amorphous phase.

#### 4. Conclusion

In summary, we studied four different semicrystalline polymers and indicated that yielding of a semicrystalline polymer below  $T_g$  involves two yielding, yielding of glassy phase and yielding of crystalline phase. Splitting of the peaks of yielding of glassy and amorphous phases is observed in the vicinity of the glass transition temperature where the imbalance between the strength of glassy phase and coherence of crystalline phase increases. We concluded that yielding of crystalline phase is the consequence of high chain tension in the amorphous phase which below  $T_g$  it requires the preceded yielding of glassy phase. Destruction of the chain networking in the amorphous phase makes it impossible to develop surviving high chain tension in that phase and exert the required force to disintegrate the crystalline domains. This paper studies mechanics of semicrystalline polymers by paying more attention to the role of amorphous phase rather than studying the crystalline phase alone.

#### Supporting Information

Supporting Information is available from the Wiley Online Library or from the author.

#### Acknowledgements

This work was supported, in part, by a grant from National Science Foundation (DMR-1905870).

#### Conflict of Interest

The authors declare no conflict of interest.

#### Keywords

molecular mechanics, polymer physics, semicrystalline polymers, yielding

Received: April 27, 2020

Revised: June 13, 2020

Published online:

- [1] S. Patlazhan, Y. Remond, *J. Mater. Sci.* **2012**, *47*, 6749.
- [2] J. V. Van Dommelen, D. Parks, M. Boyce, W. Brekelmans, F. Baaijens, *J. Mech. Phys. Solids* **2003**, *51*, 519.
- [3] A. Drozdov, R. Klitkou, J. D. Christiansen, *Mech. Mater.* **2013**, *56*, 53.
- [4] M. Jeridi, L. Laiarinandrasana, K. Sai, *Int. J. Solids Struct.* **2015**, *53*, 12.
- [5] O. Gueguen, S. Ahzi, A. Makradi, S. Belouettar, *Mech. Mater.* **2010**, *42*, 1.
- [6] S. Nikolov, I. Doghri, O. Pierard, L. Zealouk, A. Goldberg, *J. Mech. Phys. Solids* **2002**, *50*, 2275.
- [7] A. Sedighiamiri, T. Van Erp, G. Peters, L. Govaert, J. Van Dommelen, *J. Polym. Sci., Part B: Polym. Phys.* **2010**, *48*, 2173.
- [8] K. Schneider, *J. Polym. Sci., Part B: Polym. Phys.* **2010**, *48*, 1574.
- [9] K. Schneider, S. Trabelsi, N. Zafeiropoulos, R. Davies, C. Riekel, M. Stamm, *Macromol. Symp.* **2006**, *236*, 241.
- [10] G. Stoclet, J. M. Lefebvre, B. Yeniad, G. G. du Sart, S. De Vos, *Polymer* **2018**, *134*, 227.
- [11] C. Thomas, R. Seguela, F. Detrez, V. Miri, C. Vanmansart, *Polymer* **2009**, *50*, 3714.
- [12] L.-Z. Liu, B. S. Hsiao, B. X. Fu, S. Ran, S. Toki, B. Chu, A. H. Tsou, P. K. Agarwal, *Macromolecules* **2003**, *36*, 1920.
- [13] Y. Mao, D. G. Bucknall, R. M. Kriegel, *Polymer* **2018**, *143*, 228.
- [14] P. J. Flory, *Nature* **1978**, *272*, 226.
- [15] A. Peterlin, *J. Mater. Sci.* **1971**, *6*, 490.
- [16] A. Peterlin, *Colloid Polym. Sci.* **1987**, *265*, 357.
- [17] K. Hong, A. Rastogi, G. Strobl, *Macromolecules* **2004**, *37*, 10165.
- [18] K. Hong, A. Rastogi, G. Strobl, *Macromolecules* **2004**, *37*, 10174.
- [19] M. Razavi, S.-Q. Wang, *Macromolecules* **2019**, *52*, 5429.
- [20] M. Razavi, S.-Q. Wang, unpublished.
- [21] S.-Q. Wang, S. Cheng, P. Lin, X. Li, *J. Chem. Phys.* **2014**, *141*, 094905.
- [22] J. Liu, P. Lin, S. Cheng, W. Wang, J. W. Mays, S.-Q. Wang, *ACS Macro Lett.* **2015**, *4*, 1072.
- [23] J. Liu, Z. Zhao, W. Wang, J. W. Mays, S. Q. Wang, *J. Polym. Sci., Part B: Polym. Phys.* **2019**, *57*, 758.
- [24] M. Razavi, S. Cheng, D. Huang, S. Zhang, S.-Q. Wang, *Polymer* **2020**, *197*, 122445.
- [25] H.-N. Lee, K. Paeng, S. F. Swallen, M. Ediger, *Science* **2009**, *323*, 231.
- [26] G. S. Rohrer, *Structure and Bonding in Crystalline Materials*, Cambridge University Press, Cambridge, UK **2001**.
- [27] T. Smith, M. Razavi, S. Wang, *Bull. Am. Phys. Soc.* **2020**, *65*.